0026-895X/04/6503-685–691$20.00
MOLECULAR PHARMACOLOGY
Copyright © 2004 The American Society for Pharmacology and Experimental Therapeutics
Mol Pharmacol 65:685–691, 2004

Vol. 65, No. 3
2969/1132905
Printed in U.S.A.

Combinatorial Interaction of Scorpion Toxins Lqh-2, Lqh-3, and LqhαIT with Sodium Channel Receptor Sites-3

Enrico Leipold, Songqing Lu, Dalia Gordon, Alfred Hansel, and Stefan H. Heinemann

Research Unit "Molecular and Cellular Biophysics", Medical Faculty of the Friedrich Schiller University Jena, Jena, Germany (E.L., S.L., A.H., S.H.H.); and Department of Plant Sciences, Tel Aviv University, Tel Aviv, Israel (D.G.)

Received September 15, 2003; accepted December 3, 2003

This article is available online at http://molpharm.aspetjournals.org

ABSTRACT

Scorpion α-toxins LqhαIT, Lqh-2, and Lqh-3 are representatives of three groups of α-toxins that differ in their preference for insects and mammals. These α-insect, antimammalian, and α-like toxins bind to voltage-gated sodium channels and slow down channel inactivation. Sodium channel mutagenesis studies using various α-toxins have shown that they interact with receptor site 3, which is composed mainly of a short stretch of amino-acid residues between S3 and S4 of domain 4. Variation in this region results in marked differences between various subtypes of sodium channels with respect to their sensitivity to the three Lqh toxins. We incorporated the S3-S4 linker of domain 4 from $hNa_V1.2$/$hNa_V1.1$, $hNa_V1.3$, $hNa_V1.6$, and $hNa_V1.7$ channels as well as individual point mutations into the $rNa_V1.4$ skeletal muscle sodium channel. Our data show that the affinity of Lqh-3 and LqhαIT to sodium channels is markedly determined by an aspartate residue (Asp1428 in $rNa_V1.4$); when mutated to glutamate, as is present in $Na_V1.1$–1.3 channels, Lqh-3–channel interactions are abolished. The interaction of Lqh-2 and LqhαIT, however, is strongly reduced when a lysine residue (Lys1432 in $rNa_V1.4$) is replaced by threonine (as in $hNa_V1.7$), whereas this substitution is without effect for Lqh-3. The influence of Lys1432 on Lqh-2 and LqhαIT strongly depends on the context of the Asp/Glu site at position 1428, giving rise to a wide variety of toxicological phenotypes by means of a combinatorial mixing and matching of only a few residues in receptor site 3.

Voltage-gated sodium (Na_V) channels consist of a large (~260 kDa) pore-forming α-subunit, composed of four homologous domains (D1–D4), each with six transmembrane segments (S1–S6) and a hairpin-like pore region between S5 and S6. Because of their structural conservation in vertebrates and invertebrates and their pivotal role in cellular excitability, Na_V channels are targeted by a large variety of chemically distinct toxins, many of which do not differentiate among channel subtypes (Catterall, 1992; Gordon, 1997). However, some scorpion neurotoxins show specificity for insect or mammalian Na_V channels, and others are able to differentiate between Na_V subtypes in mammalian neurons (Gordon et al., 2002). This selectivity is attributed to differences of active sites on the toxins and to variations in receptor binding sites on distinct Na_V channels that, when identified, may be used for design of selective drugs.

Scorpion toxins affecting Na_V channels are 61- to 76-residue polypeptides that comprise two major classes, α- and β-toxins, according to their mode of action and binding properties to distinct sites (receptor sites-3 and -4, respectively) on Na_V channels (Martin-Eauclaire and Couraud, 1995; Gordon et al., 1998). α-Toxins inhibit Na_V channel inactivation in various excitable preparations, but they show vast differences in preference for insect and mammalian Na_V channels. Accordingly, they are divided into classic α-toxins, which are highly active in mammalian brain [e.g., Lqh-2 (*Leiurus quinquestriatus hebraeus*)]; α-toxins, which are very active in insects (e.g., LqhαIT); and α-like toxins, which are active in both the mammalian and insect central nervous system (CNS) (e.g., Lqh-3) (Gordon et al., 1996, 2002; Sautiere et al., 1998; Gilles et al., 1999, 2000a; Krimm et al., 1999).

Despite differences in toxicity and binding properties, all scorpion α-toxins bind to receptor site 3, the structural features of which are still elusive, but known to involve the extracellular loops S5–S6 of D1 and D4 (Tejedor and Catterall, 1988; Thomson and Catterall, 1989) and S3–S4 of D4 of rat $Na_V1.2$ (Catterall, 1992, 2000; Rogers et al., 1996). Mutagenesis within the external linker S3–S4 in domain 4 of rat brain $Na_V1.2$ identified a negatively charged residue, Glu1613, as a major determinant that affects the binding of a classic scorpion α-toxin (Rogers et al., 1996).

Mammalian Na_V channels are encoded by a gene family.

This work was supported by grants from the Deutsche Forschungsgemeinschaft (HE 2993/5, to S.H.H.) and in part by research grant IS-3259–01 from BARD, The United States-Israel Binational Agricultural Research and Development Fund (to D.G.).

ABBREVIATIONS: Na_V channels, voltage-gated sodium channels; CNS, central nervous system; Lqh, *Leiurus quinquestriatus hebraeus*; HEK, human embryonic kidney.

Some members are broadly expressed in the CNS ($Na_v1.1$–1.3, $Na_v1.6$), whereas the expression of others is restricted to specific tissues, such as the peripheral nervous system ($Na_v1.7$), sensory neurons ($Na_v1.8$ and $Na_v1.9$), skeletal muscle ($Na_v1.4$), and cardiac muscle ($Na_v1.5$). In most instances, neuronal Na_V channels (except $Na_v1.8$ and $Na_v1.9$) mediate tetrodotoxin-sensitive Na^+ currents and have similar electrophysiological properties. Interestingly, most neurons were found to express various Na_V channel subtypes in their cell bodies or at distinct membrane regions; such expression is plastically regulated under developmental and pathological conditions (Goldin, 1999; Catterall, 2000). The identification of these channel subtypes and elucidation of their role is technically limited and requires specific probes. Scorpion α-toxins provide a unique tool for such identification because their affinity for different channel subtypes is very diverse. For example, LqhαIT is ~2000-fold less active in mouse brain than Lqh-2 and competes only at micromolar concentrations for binding to rat brain synaptosomes. The α-like toxin, Lqh-3, is highly toxic in the mouse brain but is a very weak competitor for Lqh-2 binding to rat brain synaptosomes (Gordon et al., 1996, 2002; Gilles et al., 1999, 2000a). Moreover, Lqh-3 and LqhαIT barely affect the Na^+ current mediated by the heterologously expressed $rNa_v1.2$ in contrast to the strong inhibition of inactivation induced by Lqh-2 (Gilles et al., 1999, 2000a, 2001). Conversely, under patch-clamp conditions, Lqh-3 strongly inhibits the Na_V channel inactivation in rat CA1 pyramidal neurons in hippocampal slices, whereas Lqh-2 has no effect (Gilles et al., 1999). Thus, α-like toxins do not target the majority of Na_V channel subtypes in brain synaptosomes (e.g., $rNa_v1.2$/1.2a and most likely $rNa_v1.1$) but are active on another as-yet unidentified brain Na_V channel that is insensitive to Lqh-2. In contrast, the three α-toxins, Lqh-2, Lqh-3, and LqhαIT, similarly affect muscular Na_V channels expressed in mammalian cells (Chen et al., 1999; Gilles et al., 2000a; Chen and Heinemann, 2001). Both Lqh-2 and Lqh-3 inhibit tetrodotoxin-sensitive Na_V channel inactivation in dorsal root ganglia neurons but their effect differs prominently, suggesting that the target channels are not identical (Gilles et al., 2000a). This is corroborated by the higher affinity of Lqh-3 for the peripheral nerve channel, $hNa_v1.7$, compared with that of Lqh-2 (Chen et al., 2002). Evidently, the target Na_V channel subtype for α-like toxins in the mammalian brain and in the peripheral nervous system still needs to be elucidated.

In this study, we analyzed those Na_V channel features in the external linker S3–S4 in domain 4, which enable the selective recognition of each of the three different α-toxins. We employed two complementary approaches; the first was to construct channel chimeras, in which the S3–S4-linker of $rNa_V1.4$ (about equally sensitive to all toxins) is replaced by the amino acid variable stretch present in each of the other neuronal Na_V channel subtypes. In the second approach, site-directed mutations were introduced in the background of the wild-type and the chimeras to elucidate the role of individual residues for each toxin effect. Our results demonstrate that a single charge-conserving substitution in this linker absolutely confers channel sensitivity to Lqh-3. Other residues confer sensitivity for LqhαIT and Lqh-2 in a background-dependent manner.

Materials and Methods

Site-Directed Mutagenesis. The channel constructs used in this study were expressed from the mammalian expression vector pcDNA3. Mutations were introduced in the background of the $rNa_V1.4$ channel (Trimmer et al., 1989) in the linker between the membrane-spanning segments S3 and S4 in the fourth homologous domain of rNav1.4 using PCR-based site-directed mutagenesis. The mutants are summarized in Fig. 1. The sequences of all mutants were verified by sequence analysis. Plasmid DNA was isolated from *E. coli* using the Midi- or Maxi-plasmid purification kit (QIAGEN, Hilden, Germany).

Cell Culture and Transfection. HEK 293 cells (CAMR, Porton Down, Salisbury, UK) were maintained in 45% Dulbecco's modified Eagle's medium and 45% Ham's F12, supplemented with 10% fetal calf serum in a 5% CO_2 incubator at 37°C. HEK 293 cells were trypsinized, diluted with culture medium, and grown in 35-mm dishes. When HEK 293 cells were grown to 30 to 50% confluence, transient transfection was performed using the Superfect transfection kit (QIAGEN). HEK 293 cells were transfected with a 5:1 ratio of the Na_v channel expression plasmids and a vector encoding the CD8 antigen (Jurman et al., 1994). The cells were used for electrophysiological recordings 2 to 3 days after transfection. Dynabeads (Deutsche Dynal GmbH, Hamburg, Germany) were used for visual identification of individual transfected cells, and many bead-decorated cells expressed Na_v channels.

Electrophysiological Measurements. Whole-cell voltage-clamp experiments were performed as described previously (Chen et al., 1999). Briefly, patch pipettes with resistances of 0.9 to 2.0 MΩ were used. The series resistance was compensated for by more than 80% to minimize voltage errors. An EPC9 patch-clamp amplifier was operated by Pulse+PulseFit and PatchMaster software (both from HEKA Elektronik, Lambrecht, Germany). Leak and capacitive currents were corrected with a p/n method. Currents were low-pass filtered at 5 kHz and sampled at a rate of 25 kHz. All experiments were performed at constant temperature, 19 to 21°C. Data analysis was performed using PulseFit, PatchMaster (HEKA) and IgorPro (WaveMetrics, Lake Oswego, OR).

The patch pipettes contained 35 mM NaCl, 105 mM CsF, 10 mM EGTA, and 10 mM HEPES, pH adjusted to 7.4 with CsOH. The bath solution contained 150 mM NaCl, 2 mM KCl, 1.5 mM $CaCl_2$, 1 mM $MgCl_2$, and 10 mM HEPES, pH adjusted to 7.4 with NaOH. The

Channel type, mutant name	Residue number	S3(D4)											
$Na_V1.4$, µI, SkM1	1423	G	L	A	L	S	D	L	I	Q	K	Y	F
$hNa_V1.2$, Brain I+II	1608		M	F		A	E			E			
$hNa_V1.3$, hBrain III, rPN1	1554		M	F		A	E	M		E			
$hNa_V1.6$, Scn8a, NaCh6	1598		M	F		A		I		E			
$hNa_V1.7$, hPN1	1581		M	F		A				E	T		
$Na_V1.4$_DtoE							E						
$Na_V1.2$_EtoD			M	F		A				E			
$Na_V1.7$_DtoE			M	F		A	E			E	T		
$Na_V1.4$_QtoE										E			
$Na_V1.4$_KtoT											T		
$Na_V1.4$_LA-StoMF-A			M	F		A							

Fig. 1. Receptor site 3 in S3/4(D4) for various Na_V channel subtypes and mutants used in this study. Alignment of the major component of toxin receptor site 3 (i.e., the linker between S3 and S4 in domain 4). The part of the sequence belonging to S3(D4) is highlighted by vertical lines. The first five sequences show the residues found in $Na_V1.4$ [here considered wild type (wt)], $Na_V1.2$/$Na_V1.1$, human $Na_V1.3$ (or rat $Na_V1.7$), $Na_V1.6$, and human $Na_V1.7$. The sequences of the indicated neuronal Na_V channels were inserted into $rNa_V1.4$. In addition, individual residues or groups of residues were exchanged, giving rise to the mutants listed in the last six rows. Negatively charged residues are highlighted in dark gray, positive residues in light gray.

application of toxin was performed with an application pipette as described previously (Chen et al., 1999).

Activation. From a holding potential of −120 mV, test depolarizations in the range from −80 to +60 mV in steps of 10 mV were applied at an interval of 5 s. The peak currents were fit with a Hodgkin-Huxley activation formalism involving $m = 3$ activation gates and a single-channel characteristics according to Goldman-Hodgkin-Katz.

$$I_{peak}(V) = \frac{I_{max}}{(1 + e^{-(V - V_m)/K_m})^3}$$

$$I_{max} = \Gamma V \frac{1 - e^{-(V - E_{rev})/25\ mV}}{1 - e^{-V/25\ mV}} \quad (1)$$

V_m is the voltage of half-maximal gate activation, k_m is the corresponding slope factor, Γ is the maximal conductance of all channels, and E_{rev} is the reversal potential.

Voltage Dependence of Fast Inactivation. From a holding potential of −120 mV, cells were conditioned for 500 ms at voltages ranging from −120 to −25 mV in steps of 5 mV. Subsequently, peak current was determined at −20 mV. The repetition interval was 10 s. The peak current plotted versus the conditioning voltage was described with a Boltzmann function.

$$I(V) = \frac{I_{min}}{(1 + e^{-(V - V_h)/k_h})} \quad (2)$$

with the half-maximal inactivation voltage V_h and the corresponding slope factor k_h that indicates the voltage dependence of steady-state fast inactivation.

Toxin Dependence of Fast Inactivation. Currents were recorded in the absence and the presence of several toxin concentrations. The degree of fast inactivation was assayed at 0 mV by measuring the peak current as well as the mean current level between 4.5 and 5 ms after the start of the depolarization. This ratio $I_{5\ ms}/I_{peak}$ gives an estimate of the probability for the channels not to be inactivated after 5 ms; a value of zero represents complete inactivation within 4.5 ms and a value of 1 represents no inactivation. The dose dependence for toxin-induced removal of fast inactivation was measured by plotting $I_{5\ ms}/I_{peak}$ as a function of toxin concentrations. The concentration dependence was described with the Hill equation.

$$\frac{I_{5\ ms}}{I_{peak}}(0\ mV) = a_0 + \frac{a_1}{1 + \left(\frac{EC_{50}}{[toxin]}\right)^{n_H}} \quad (3)$$

where n_H is the Hill coefficient, [toxin] is the toxin concentration, and a_0 is the offset. The amplitude, a_1 plus a_0, provides the maximal value of $I_{5\ ms}/I_{peak}$ at 0 mV indicating the expected maximal effect of the toxin on fast inactivation. EC_{50} provides a measure for the concentration of half-maximal inhibition of fast inactivation. For data fits, the a_0 values always were held to the values obtained under control conditions. To reduce variability, h was set to 1 in all cases. Because even high toxin concentrations did not result in a full α-toxin effect for some mutants, $a_0 + a_1$ was set to a constant value (0.75) for all dose-response fits. Data points were weighted according to the standard error of the mean; error estimates for EC_{50} values were obtained from these fits with the IgorPro program.

All data were presented as mean ± S.E.M. (n = number of independent experiments). Significance of differences between two groups of data were tested with a two-sided Student's t test.

Results

Receptor site 3 of voltage-gated sodium channels is largely determined by the extracellularly accessible loop between segments 3 and 4 of domain 4. Interestingly, although most parts of the core domains of Na_V channels are rather conserved, there is considerable variability in this region among mammalian sodium channels (Fig. 1). In addition, various α-toxin groups have different effects on the same Na_V channel; e.g., whereas Lqh-2 is very active on $Na_V1.2$ channels, Lqh-3 is almost inactive (Chen et al., 2002). To gain insight into the molecular mechanisms underlying the mutual toxin-channel specificity, we applied a mutagenesis approach. Based on the rat $Na_V1.4$ channel, which is similarly sensitive to the three groups of α-toxins, we replaced the S3–S4 linker in domain 4 by its counterparts present in various Na_V channel subtypes and examined the effects of the three different α-toxins on each channel mutant. Starting from $Na_v1.4$ wild-type channels, we first introduced receptor sites from the human neuronal channels $Na_V1.1$/$Na_V1.2$ (in the putative receptor site 3, these channels are identical), $Na_V1.3$, $Na_V1.6$, and $Na_V1.7$. Note that the sequences of receptor site 3 of human $Na_V1.3$ and rat $Na_V1.7$ are identical (Fig. 1). In addition, we generated channel mutants in which, based on the background receptor site 3, sequences of $Na_V1.2$-, $Na_V1.4$-, and $hNa_V1.7$-specific residues or groups of residues were replaced by others. In particular, we applied this approach to specifically test the influence of residues Asp1428, Gln1431, and Lys1432 (residue numbers of $rNa_V1.4$).

Functional Parameters of Mutated Na_V Channels. All these mutants were expressed in HEK 293 cells giving rise to functional Na_V channels. The mutations had no impact on the current densities obtained. The function of the mutated Na_V channels was assayed by measuring and analyzing current-voltage relationships and steady-state inactivation. Sample data for channel activation are shown in Fig. 2A. The half-maximal activation voltage V_m and the slope factors k_m for all mutants are plotted in Fig. 2C; variations for V_m were within ±4 mV and for k_m within ±1 mV. Thus, no big changes in activation parameters were detected, implying that alterations of receptor site 3 have only a marginal impact on the channel-activating movement of the S4 segment in domain 4.

Steady-state inactivation after 500-ms conditioning was described by a single Boltzmann function. The resulting half-maximal inactivation voltages V_h and the slope factors k_h are also shown in Fig. 2C. Again, for most mutants the variation of V_h was within ±4 mV and the variation for k_h within ±1 mV. However, the resulting V_h for mutant $Na_v1.3$ was shifted by about −20 mV with respect to the wild type (−73.9 ± 0.7 mV, $n = 43$ for $Na_V1.4$; −93.4 ± 0.8, $n = 37$ for mutant $hNa_V1.3$, $P \ll 0.001$). This shift can be attributed to the residue exchange L1429M, because this is the only difference between mutants $hNa_V1.3$ and $Na_V1.2$ ($V_h = -76.0 \pm 0.7$, $n = 48$, $P \ll 0.001$). The slope factors were not affected. The shift in V_h did not result from a contribution of slow inactivation, because similar experiments using conditioning pulses of 50 ms also resulted in such a shift, whereas protocols assaying slow inactivation (with 5-s conditioning) did not show shifts (data not shown). Besides this effect of mutant $hNa_V1.3$, all other mutants show inactivation parameters indistinguishable from that of wild type. Therefore, altered gating properties did not contaminate the subsequent assessment of toxin effects—this is an important prerequisite, because the effects of scorpion α-toxins are state- and voltage-dependent. In addition, it is noteworthy that even substantial nonconservative mutagenesis of receptor site 3

does not affect channel inactivation, even though toxin binding to that site has a strong effect on inactivation.

Receptor Site 3 Chimeras. In a first screening, all mutants were tested with regard to the effect of 20 nM Lqh-3, LqhαIT, and Lqh-2. In Fig. 3 sample traces at −20 mV are shown for those mutants harboring receptor sites-3 of other neuronal channel types. First, it is evident that mutagenesis does not influence kinetics of fast inactivation; this is also true for all other mutants not shown in Fig. 2. Upon application of 20 nM of Lqh-3, LqhαIT, and Lqh-2, inactivation is strongly impaired in wild-type $Na_V1.4$ channels, almost reaching saturation (Fig. 2, top row). Mutagenesis of receptor site 3 has a differential impact on the three toxins' effects. Whereas mutants $Na_V1.2$ and $hNa_V1.3$ are basically insensitive to Lqh-3 and only weakly sensitive to LqhαIT, there is only a small effect on the activity of Lqh-2. Mutation $Na_V1.6$ only weakly influences the effect of all toxins. Unexpectedly, for mutant $hNa_V1.7$ the strongest effect is obtained for the activity of LqhαIT, followed by Lqh-2 and Lqh-3. Thus, variation in the structure of receptor site 3 among neuronal Na_V channels modulates the action of the three α-toxins in a complex manner, as suggested by the native channels $Na_V1.2$/$Na_V1.7$ and Lqh-3/Lqh-2 (Chen et al., 2002).

On the one hand, this raises the possibility of using these toxins for the identification of specific Na_V channel subtypes present in various neurons. On the other hand, the variability obtained by the exchange of only a few residues in a constant background (of $Na_V1.4$) provides an ideal basis for a more detailed characterization of the molecular determinants responsible for the mutual toxin–channel recognition sites. Therefore, we constructed conservative mutants in which only single residues (or groups) were exchanged on the basis of $Na_V1.4$ or of one of the site 3 swap mutants (see Fig. 1).

Single-Site Mutants. For all mutants, the toxin effects were assayed quantitatively by applying different toxin concentrations to compile dose-response relationships. In Fig. 4, such dose-response data are shown for a selection of mutants together with the superimposed fit results. The maximal effect obtained with application of active α-toxins depends mainly on the linker between domains 3 and 4 as well as the regions forming the receptor for the inactivation domain. Therefore, we assume that mutation of the extracellularly accessible receptor site 3 does not alter the theoretically obtainable toxin effect (i.e., the residual speed of inactivation upon toxin saturation). Hence, we constrained the dose-response fits to a maximal $a_0 + a_1$ value (see eq. 3) of 0.75. The Hill coefficients were set to unity, such that the data could be described by the EC_{50} values as the only free parameter. The resulting EC_{50} values of all mutants investigated are listed in Table 1.

All data are listed in Table 1, but the results are not easily extracted. Therefore, we show in Fig. 5 on a logarithmic scale the relative impact of specific mutations on the effects of all three toxins. The data are grouped according to the site of interest. Most remarkable is mutation D1428E. For Lqh-3, it seems to be a necessary criterion to have an aspartate at position 1428 in receptor site 3. Mutagenesis to glutamate (only a CH_2-group difference from aspartate) results in a reduction of >1000-fold in Lqh-3 effect. In contrast, this mutation has no impact at all for Lqh-2. In the background of receptor site 3 of $hNa_V1.7$ (i.e., in the presence of Thr1432), the exchange D1428E even increases the effect of Lqh-2. For LqhαIT, the situation is somewhat intermediate: whereas D1428E has a very strong impact in the background of $Na_V1.4$ wild-type and mutant $Na_V1.2$ (i.e., in the presence of Lys1432), it does not change the activity of LqhαIT in the

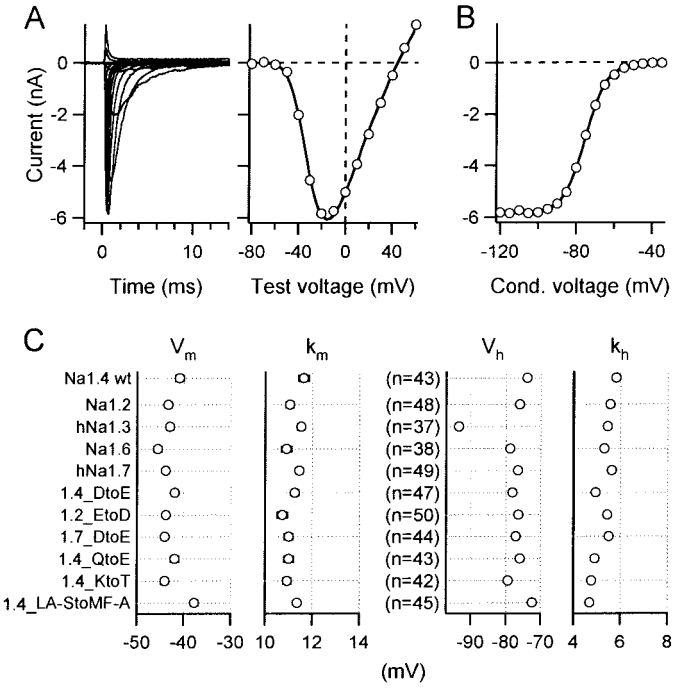

Fig. 2. A, sample current-voltage relationship of $rNa_V1.4$ channels expressed in HEK 293 cells. From a holding potential of −120 mV, step-depolarizations ranging from −80 to +60 mV in steps of 10 mV were applied; the resulting current traces are shown superimposed, low-pass filtered at 5 kHz (left). The peak currents were plotted as a function of the test potential to yield current-voltage relationships (right). These were fit with eq. 1, yielding the half-maximal activation voltage per V_m and the slope factor k_m. B, sample steady-state inactivation curve, fit with a first-order Boltzmann function (eq. 2), yielding the half-maximal inactivation voltage V_h and the slope factor k_h. C, steady-state activation and inactivation parameters for all mutants.

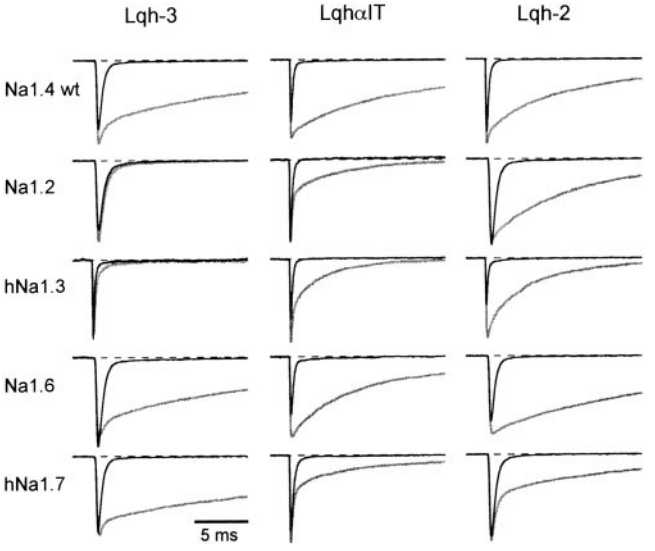

Fig. 3. Sample current traces of mutants with receptor sites-3 resembling the indicated neuronal channel types at −20 mV before (black) and after application of 20 nM of the indicated toxin (gray).

background of hNa$_V$1.7 (i.e., in the presence of Thr1432). Thus, Lqhα IT behaves like Lqh-3 with Lys1432 and like Lqh-2 with Thr1432. Notably, the affinity of Lqhα IT strongly depends on both residues Asp1428 and Lys1432 in Na$_V$1.4, whereas that of Lqh-3 depends mainly on Asp1428. In other words, Lqh-3 action seems to be independent from the residue at position 1432, whereas the other two toxins depend strongly on the nature of this residue.

This rather indirect inference is directly shown in the next group of data, captioned "K1432T". As expected, the Lqh-3 effect does not strongly depend on whether there is a lysine or a threonine at position 1432. However, the effects of Lqhα IT (and, to a lesser extent, Lqh-2) are reduced when Lys1432 is mutated to Thr. However, this is true only in the background of a receptor site 3 harboring Asp1428. In summary, the channel sensitivity to Lqh-3 is determined mainly by the Asp/Glu exchange at position 1428 in receptor site 3. Lqhα IT recognizes D1428E only in the presence of Lys1432 and Lqh-2 only in the presence of Thr1432. Both Lqhα IT and Lqh-2 recognize K1432T only in the background of Asp1428.

The conservative changes at positions Leu1429 (to Ile or Met) and LA-S1424MF-A have only small impacts on the effects of Lqh toxins. Q1431E, however, leaves the effects of Lqh-3 and Lqhα IT unchanged, whereas it decreases the effect of Lqh-2. This differential modulation is seen only in the background of the Na$_V$1.4 channel; when receptor site 3 is more neuronal-like (i.e., with MF-A1424 in place of LA-S), mutation Q1431E has only a marginal impact on all three toxins. Thus, also in this case, individual parts of receptor site 3 are of very differential importance for the association of the three Lqh toxins—and this in a context-dependent manner.

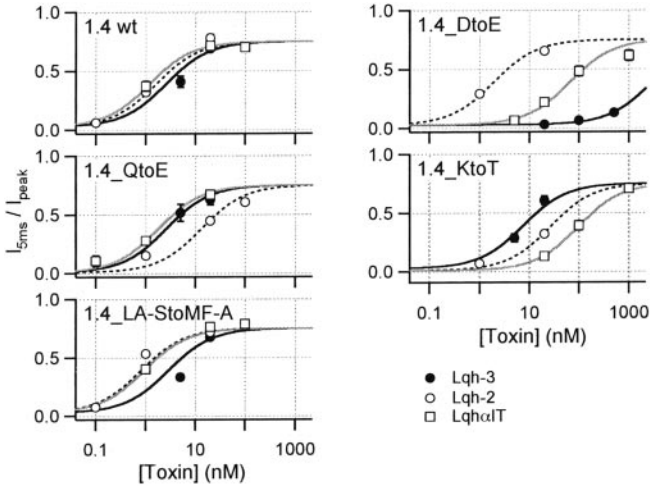

Fig. 4. Selection of dose-response relationships for Lqh-3 (black), Lqhα IT (gray), and Lqh-2 (dashed). For data fits according to eq. 3, the maximal value was fixed to 0.75 and the Hill coefficient to 1.0.

TABLE 1
EC$_{50}$ values derived from dose-response curves shown in Fig. 4

Mutant	Lqh-3	Lqhα IT	Lqh-2
		nM	
rNa$_V$1.4, wt	1.83 ± 0.25	1.19 ± 0.24	1.64 ± 0.16
Na$_V$1.2 (Na$_V$1.1)	1840 ± 173	20.6 ± 0.9	0.969 ± 0.071
hNa$_V$1.3 (rNa$_V$1.7)	3890 ± 1110	190 ± 11	2.35 ± 0.29
Na$_V$1.6	9.48 ± 0.82	0.247 ± 0.041	0.778 ± 0.058
hNa$_V$1.7	6.22 ± 0.64	50.8 ± 5.2	7.00 ± 1.15
Na$_V$1.4_DtoE	2980 ± 282	65.7 ± 6.1	1.92 ± 0.23
Na$_V$1.2_EtoD	5.52 ± 0.56	0.338 ± 0.028	0.53 ± 0.08
Na$_V$1.7_DtoE	2290 ± 220	42.1 ± 4.0	1.56 ± 0.15
Na$_V$1.4_QtoE	2.59 ± 0.89	1.80 ± 0.25	13.2 ± 1.1
Na$_V$1.4_KtoT	7.46 ± 1.21	96.1 ± 7.9	26.2 ± 2.7
Na$_V$1.4_LA-StoMF-A	2.88 ± 0.22	0.934 ± 0.169	0.804 ± 0.054

Discussion

Functional Impacts of Receptor Site 3 Mutagenesis. In this study, we assayed various Na$_V$1.4 channel types that were mutated in the S3–S4 linker of domain 4. None of these mutants showed strong alterations in the voltage dependence of activation. This is consistent with a minor role of domain 4 for channel activation (Chahine et al., 1994; Chen et al., 1996). In addition, most mutants did not alter the inactivation properties either. This is surprising because binding of α-toxins to that site has a strong impact on channel inactivation. An exception is mutation L1429M, which leads to a clear shift in steady-state inactivation to more hyperpolarizing potentials, indicating a stabilized inactivated state. This can be explained molecularly by a coupling of voltage-sensor movement in domain 4 and fast inactivation (Catterall, 2002). However, at present, we cannot determine whether the particular site 1429 is necessary for transmitting effects on channel inactivation or the nature of the introduced residue (here methionine) is important. It is interesting to note,

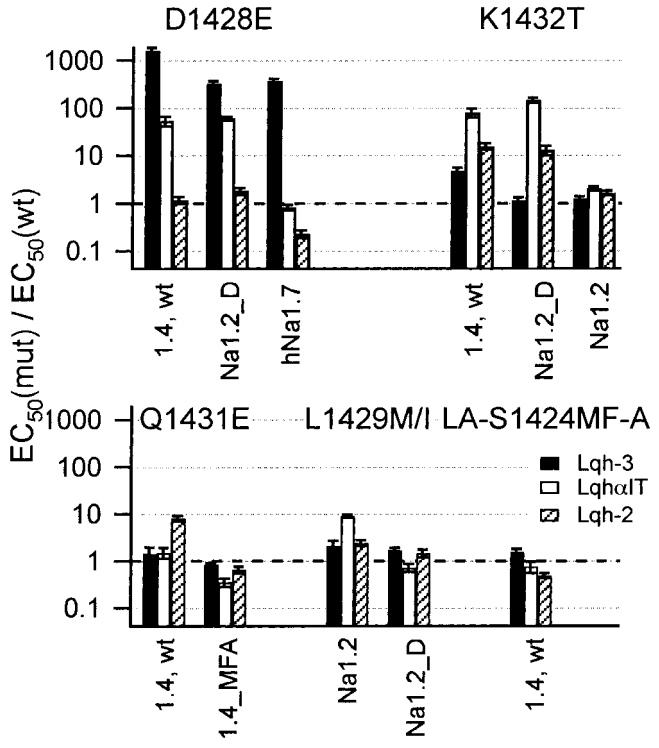

Fig. 5. Relative change in apparent EC$_{50}$ values introduced by the indicated mutations. The data are grouped according to the site of mutagenesis (e.g., Arg1428). The small labeling of the histogram bars indicates the background used for mutagenesis (e.g., "Na1.2" under "K1432T" means that Thr1432 was introduced in the background of rNa$_V$1.4 mutant "Na$_V$1.2"; i.e., "Na$_V$1.7_DtoE") (see Table 1). The shading of the histogram bars indicates the toxins: Lqh-3 (black), Lqhα IT (white), Lqh-2 (hatched). For this sequence of toxins, the ratio values for the most relevant mutations are as follows: D1428E: Na$_V$1.4, wt: 1633, 55.0, 1.18; Na1.2_EtoD: 333, 60.9, 1.82; hNa1.7: 368, 0.828, 0.223; K1432T: Na$_V$1.4, wt: 4.88, 80.5, 16.0; Na1.2_EtoD: 1.13, 150, 13.1; Na1.2: 1.24, 2.04, 1.61.

however, that $hNa_V1.3$ and $rNa_V1.7$ channels are unique in harboring a methionine residue at that position.

The different effects of mutations in the S3–S4 linker in domain 4 of Na_V channels on the affinity of each of the three Lqh α-toxins suggest that they bind to receptor site 3 in different fashions. Although all the distinct α-toxins interact with residues in this short linker, they may bind to partially overlapping sites, which may depend on the functional surface of each toxin. Moreover, because the impact on the affinity of Lqh-2, the most potent anti-mammalian α-toxin, by two mutations, Lys to Thr and Gln to Glu, was relatively small (Fig. 5 and Table 1), it is conceivable that other parts of the channel may be involved in formation of receptor site 3 and in the high affinity of Lqh-2 to most mammalian Na_V channels. This assumption is supported by the low affinity of Lqh-2 to insect Na_V channels, which are practically identical to the mammalian $Na_V1.6$ in the S3–S4 region in domain 4, to which Lqh-2 reveals high affinity (Table 1).

Use of Lqh Toxins for Identifying Na_V Channels. The combinatorial use of Lqh toxins provides a tool for identifying neuronal Na_V channel types. Although in some cases there is still some uncertainty about whether the site 3 swap confers the full toxin-binding properties of the respective wild types, the discriminative power of the three Lqh toxins, particularly when used in combination, will be very helpful in targeting specific Na_V channels, either for research purposes or for pharmacological applications. Fluorescent labeling of these toxins as performed for other, less specific α- and β-toxins (Massensini et al., 2002) may provide further insight into Na_V channel distributions in nervous tissues.

Limitations in Drawing Toxicological Conclusions for Humans Based on Animal Experiments. Receptor site 3 mainly determines the mode by which Na_V channels interact with scorpion α-toxins. However, toxicological studies using laboratory animals may yield results that are not easily transferred to the human system. Herein, we show that receptor site 3 of $hNa_V1.3$ channels is identical to the site of rat $Na_V1.7$ channels. The site of rat $Na_V1.3$ channels is identical to those of $Na_V1.1$ and $Na_V1.2$ channels. Thus, with respect to Lqh-3 rat and human $Na_V1.7$ channels are expected to behave in a completely different manner (factor of about 1000); therefore, rat $Na_V1.7$ channels are not suitable as models for their human orthologs.

Combinatorial Determination of Toxin-Channel Specificity. The strong diversity of functional effects exerted by the three Lqh toxins studied must be reflected in their molecular structure. Particularly intriguing is the molecular basis that allows for a very sensitive discrimination of glutamate versus aspartate in the receptor site, as shown for Lqh-3.

Thus far, the bioactive surfaces of two α-toxins were investigated systematically: LqhαIT (α-insect toxin; Tugarinov et al., 1997; Zilberberg et al., 1997) and BmK-M1 (α-like toxin; Wang et al., 2003). Mutagenesis of LqhαIT revealed that Tyr21 (Gilles et al., 2000b) and Arg64 (Tugarinov et al., 1997; Zilberberg et al., 1997) might be important for the interaction with Na_V channels. Other residues that might be part of the bioactive surface are Tyr10, Phe17, Lys8, Arg18, and Arg62 (Zilberberg et al., 1997). Site-directed mutagenesis of BmK-M1 showed that Lys62 and His64 together with Lys8 form a unique tertiary arrangement that may directly interact with receptor site 3 on the Na_V channel surface (Wang et al., 2003). These findings are consistent with a second mutagenesis approach on BmK-M1 in which aromatic residues (Tyr5, Tyr35, Trp38, Tyr42, Trp47) affected toxin properties, most likely by structural stabilization (Sun et al., 2003). The functional importance of residues that are located in a turn near the N terminus (8–10) was shown in a chimeric approach between LqhαIT and BotXIV, an α-like toxin (Bouhaouala-Zahar et al., 2002). All together, it is generally accepted that the so-called five-residue turn (residues 8–12 in the Lqh toxins used here) together with the C-terminal end of the toxins forms the channel interaction site.

At least two of the three Lqh toxins used in this study differentiate effectively between Asp1428 and Glu1428 in the background of $Na_V1.4$ channels. Together with the finding that a positive surface potential of α-toxins may correlate with their binding affinity to Na_V channels (Zilberberg et al., 1997; Krimm et al., 1999), one can speculate that positively charged residues on the toxin surface should be in physical contact with negatively charged residues in receptor site 3. The lack of positive charges in the five-residue turn in Lqh-2 and Lqh-3 highlights the C-termini with the Lys/Arg and His/Arg moieties as excellent candidates for harboring the critical interaction site. More mutagenesis studies combined with double cycle analysis are needed to clarify this point.

Because the Lys/Thr sites at position 1432 in receptor site 3 determines how strongly the Lqh toxins (in particular Lqh-2 and LqhαIT) depend on the Asp/Glu residues at position 1428, it will be important to elucidate the direct interaction partner on the bioactive surface of the toxins. Only then can the combinatorial and nonadditive contribution of these residues on toxin binding be understood on a molecular level. However, comparison of the Lqh-2, Lqh-3, and LqhαIT sequences does not readily suggest a candidate for a direct interaction partner for the Lys/Thr site of receptor site 3. Therefore, rather than examining single toxin mutants, a chimeric approach using Lqh-2 and Lqh-3 might be the strategy of choice for solving this problem.

In summary, the individual residues in receptor site 3 do not add linearly to the binding strength of Lqh toxins; rather, they give rise to a combinatorial mixing and matching of toxins and channel subtypes. As a result, simply recombining a few amino acid residues in receptor site 3 of voltage-gated sodium channels generates a very wide variety of toxicological phenotypes.

Acknowledgments

We thank A. Roßner and S. Arend for technical assistance and Dr. P. Sautière for his generous gift of scorpion α-toxins.

References

Bouhaouala-Zahar B, Benkhalifa R, Srairi N, Zenouaki I, Ligny-Lemaire C, Drevet P, Sampieri F, Pelhate M, El Ayeb M, et al. (2002) A chimeric scorpion α-toxin displays de novo electrophysiological properties similar to those of α-like toxins. *Eur J Biochem* **269:**2831–2841.

Catterall WA (1992) Cellular and molecular biology of voltage-gated sodium channels. *Physiol Rev* **72**(4 Suppl)**:**S15–S48.

Catterall WA (2000) From ionic currents to molecular mechanisms: the structure and function of voltage-gated sodium channels. *Neuron* **26:**13–25.

Catterall WA (2002) Molecular mechanisms of gating and drug block of sodium channels. *Novartis Found Symp* **241:**206–218; discussion 218–232.

Chahine M, George AL Jr, Zhou M, Ji S, Sun W, Barchi RL, and Horn R (1994) Sodium channel mutants in paramyotonia congenita uncouple inactivation from activation. *Neuron* **12:**281–294.

Chen H, Gordon D, and Heinemann SH (1999) Modulation of cloned skeletal muscle Na channels by the scorpion toxins Lqh II, Lqh III and LqhαIT. *Pflueg Arch Eur J Physiol* **439:**423–432.

Chen H and Heinemann SH (2001) Interaction of scorpion α-toxins with cardiac

sodium channels: binding properties and enhancement of slow inactivation. *J Gen Physiol* **117:**505–518.

Chen H, Lu SQ, Leipold E, Gordon D, Hansel A, and Heinemann SH (2002) Differential sensitivity of recombinant sodium channels from the central and peripheral nervous system to the scorpion toxins Lqh-2 and Lqh-3. *Eur J Neurosci* **16:**767–770.

Chen LQ, Santarelli V, Horn R, and Kallen RG (1996) A unique role for the S4 segment of domain 4 in the inactivation of sodium channels. *J Gen Physiol* **108:**549–556.

Gilles N, Blanchet B, Shichor I, Zaninetti M, Lotan I, Bertrand D, and Gordon D (1999) A scorpion α-like toxin active on insects and mammals reveals an unexpected specificity and distribution of sodium channel subtypes in rat brain neurons. *J Neurosci* **19:**8730–8739.

Gilles N, Chen HJ, Wilson H, LeGall F, Montoya G, Molgo J, Schönherr R, Nicholson G, Heinemann SH, and Gordon D (2000a) Scorpion α- and α-like toxins differentially interact with sodium channels in mammalian CNS and periphery. *Eur J Neurosci* **12:**2823–2832.

Gilles N, Krimm I, Bouet F, Froy O, Gurevitz M, Lancelin JM, and Gordon D (2000b) Structural implications on the interaction of scorpion α-like toxins with the sodium channel receptor site inferred from toxin iodination and pH-dependent binding. *J Neurochem* **75:**1735–1745.

Gilles N, Leipold E, Chen HJ, Heinemann SH, and Gordon D (2001) Effect of depolarization on binding kinetics of scorpion α-toxin highlights conformational changes of rat brain sodium channels. *Biochemistry* **40:**14576–14584.

Goldin AL (1999) Diversity of mammalian voltage-gated sodium channels. *Ann NY Acad Sci* **868:**38–50.

Gordon D, Gilles N, Bertrand D, Molgò J, Nicholson GM, Sauviat MP, Benoit E, Shichor I, Lotan I, Gurevitz M, et al. (2002) Scorpion toxins differentiating among neuronal sodium channel subtypes: nature's guide for design of selective drugs, in *Perspectives in Molecular Toxinology* (Ménez A ed) pp 215–238, Wiley and Sons, Chichister, England.

Gordon D (1997) Sodium channels as targets for neurotoxins: mode of action and interaction of neurotoxins with receptor sites on Na channels, in *Toxins And Signal Transduction* (Gutman Y and Lazarovici P eds) pp 119–149, Cellular and Molecular Mechanisms of Toxin Action, Vol. 1, Harwood Academic Press, Amsterdam.

Gordon D, Martin-Eauclaire MF, Cestele S, Kopeyan C, Carlier E, Khalifa RB, Pelhate M, and Rochat H (1996) Scorpion toxins affecting sodium current inactivation bind to distinct homologous receptor sites on rat brain and insect sodium channels. *J Biol Chem* **271:**8034–8045.

Gordon D, Savarin P, Gurevitz M, and Zinn-Justin S (1998) Functional anatomy of scorpion toxins affecting sodium channels. *J Toxicol Toxin Rev* **17:**131–159.

Jurman ME, Boland LM, Liu Y, and Yellen G (1994) Visual identification of individual transfected cells for electrophysiology using antibody-coated beads. *Biotechniques* **17:**876–881.

Krimm I, Gilles N, Sautiere P, Stankiewicz M, Pelhate M, Gordon D, and Lancelin JM (1999) NMR structures and activity of a novel alpha-like toxin from the scorpion *Leiurus quinquestriatus hebraeus*. *J Mol Biol* **285:**1749–1763.

Martin-Eauclaire MF and Couraud F (1995) Scorpion neurotoxins: effects and mechanisms, in *Handbook of Neurotoxicology* (Chang LW and Dyer RS eds) pp 688–722, Marcel Dekker, New York.

Massensini AR, Suckling J, Brammer MJ, Moraes-Santos T, Gomez MV, and Romano-Silva MA (2002) Tracking sodium channels in live cells: confocal imaging using fluorescently labeled toxins. *J Neurosci Methods* **166:**189–196.

Rogers JC, Qu Y, Tanada TN, Scheuer T, and Catterall WA (1996) Molecular determinants of high affinity binding of α-scorpion toxin and sea anemone toxin in the S3–S4 extracellular loop in domain IV of the Na^+ channel α subunit. *J Biol Chem* **271:**15950–15962.

Sautiere P, Cestele S, Kopeyan C, Martinage A, Drobecq H, Doljansky Y, and Gordon D (1998) New toxins acting on Na channels from the scorpion *Leiurus quinquestriatus hebraeus* suggest a clue to mammalian vs insect selectivity. *Toxicon* **36:**1141–1154.

Sun YM, Bosmans F, Zhu RH, Goudet C, Xiong YM, Tytgat J, and Wang DC (2003) Importance of the conserved aromatic residues in the scorpion α-like toxin BmK M1: the hydrophobic surface revisited. *J Biol Chem* **278:**24125–24131.

Tejedor FJ and Catterall WA (1988) Site of covalent attachment of α-toxin derivatives in domain I of the sodium channel α subunit. *Proc Natl Acad Sci USA* **85:**8742–8746.

Thomson WJ and Catterall WA (1989) Localization of the receptor site for α-scorpion toxins by antibody mapping: implications for sodium channel topology. *Proc Natl Acad Sci USA* **86:**10161–10165.

Trimmer JS, Cooperman SS, Tomiko SA, Zhou JY, Crean SM, Boyle MB, Kallen RG, Sheng ZH, Barchi RL, Sigworth FJ, et al. (1989) Primary structure and functional expression of a mammalian skeletal muscle sodium channel. *Neuron* **3:**33–49.

Tugarinov V, Kustanovich I, Zilberberg N, Gurevitz M, and Anglister J (1997) Solution structure of a highly insecticidal recombinant scorpion α-toxin and a mutant with increased activity. *Biochemistry* **36:**2414–2424.

Wang CG, Gilles N, Hamon A, Le Gall F, Stankiwicz M, Pelhate M, Xiong YM, Wang DC, and Chi CW (2003) Exploration of the functional site of a scorpion alpha-like toxin by site directed mutagenesis. *Biochem* **42:**4699–4707.

Zilberberg N, Froy O, Loret E, Cestéle S, Arad D, Gordon D, and Gurevitz M (1997) Identification of structural elements of a scorpion α-neurotoxin important for receptor site recognition. *J Biol Chem* **272:**14810–14816.

Address correspondence to: Prof. Dr. Stefan H. Heinemann, Molecular and Cellular Biophysics, Friedrich Schiller University Jena, Drackendorfer Str. 1, D-07747 Jena, Germany. E-mail: stefan.h.heinemann@uni-jena.de